INDIAN JOURNAL OF SCIENCE AND TECHNOLOGY

RESEARCH ARTICLE

OPEN ACCESS

Received: 19-08-2024

Accepted: 30-10-2024

Published: 10-12-2024

Citation: Navale AV, Turkane SD, Ladhane KB, Solanki CH, Sawant VA (2024) Analysis of Pile Group in Square Arrangement Embedded in Clayey Soil. Indian Journal of Science and Technology 17(45): 4765-4777. https://doi.org/10.17485/IJST/v17i45.2685

* **Corresponding author**.

navaleav@yahoo.com

Funding: None

Competing Interests: None

Published By Indian Society for Education and Environment (iSee)

ISSN
Print: 0974-6846
Electronic: 0974-5645

Analysis of Pile Group in Square Arrangement Embedded in Clayey Soil

Avinash V Navale[1]*, Sagar D Turkane[2], Kiran B Ladhane[3], Chandresh H Solanki[4], Vishwas A Sawant[5]

1 Assistant Professor, Department of Civil Engineering, Amrutvahini College of Engineering, Sangamner, 422605, Maharashtra, India
2 Assistant Professor, Department of Civil Engineering, Sandip Institute of Technology and Research Centre, Nashik, Maharashtra, India
3 Head of Department, Department of Civil Engineering, Government Polytechnic, Nashik, Maharashtra, India
4 Professor, Department of Civil Engineering, SVNIT Surat, Gujrat, India
5 Professor, Department of Civil Engineering, Indian Institute of Technology Roorkee, Roorkee, Uttarakhand, India

Abstract

Objective: The purpose of this study is to simulate and compare the response of the 3 × 3 pile group, embedded in clay, subjected to static lateral load, in terms of lateral deflection when soil is represented by different elastoplastic yield criteria. The effect of geometrical and material parameters is also investigated. **Methods:** In the developed finite element formulation, 20 node isoparametric elements have been used to model piles and pile caps. Surrounding soil has been modeled using 8-node isoparametric elements. The code is being developed in FORTRAN 90. **Findings:** The parametric study revealed the impact of the constitutive model to represent soil, pile spacing, pile length, pile diameter, and soil properties on the lateral deflection of the pile group. Mohr-Coulomb criterion predicts the lowest lateral displacement and maximum bending moment. An increase in spacing-to-diameter ratio from 2 to 6 causes a decrease in pile displacement by 80.13% in Von Misses, 70.3% in Drucker-Prager outer, 76.68% in Drucker-Prager inner, and 56.62% in Mohr-Coulomb yield criteria. An increase in the elastic modulus of soil from 20000 kPa to 60000 kPa results in a reduction in lateral displacement by 43.12% and an increase in pile diameter from .6 m to 1.0 m causes a reduction in lateral displacement by 82.73% when Von Mises criterion is used. The change in length-to-diameter ratio from 10 to 25 reduces pile displacement by 23.91%. **Novelty:** Among the Von – Mises, Mohr-Coulomb, Drucker–Prager (outer), and Drucker–Prager (inner) criteria, the Mohr-Coulomb criterion predicts the lowest lateral response for the 3 × 3 pile group. However, as the s/D ratio increases from 2 to 6, the difference in response is minimized. A marginal difference is found at the L/D ratio of more than 15. **Applications:** The developed three-dimensional finite element software can be used by pile designers to predict the response of laterally loaded pile groups.

Keywords: Lateral load; Pile group; Pile spacing; Von Misses criterion; Mohr-Coulomb criterion; Drucker-Prager criterion; Lateral pile deflection

1 Introduction

Generally, pile foundations are provided when good strata are not available at less depth and shallow foundations are not sufficient. Many onshore tall structures like tall buildings and towers are subjected to considerable wind load which transmits lateral load at foundations. Bridge structures also experience lateral load due to vehicular movements. Pile foundations are the obvious choice for them. Due to the increased energy demand, people have started exploring more applications like wind turbines and oil platforms in the ocean. Marine sea beds have been observed to have a significant presence of marine clay in many locations. Most marine structures need to be supported on pile foundations due to prevailing environmental conditions. The combined action of wave and wind forces causes a significant amount of lateral pressure on pile foundations supporting offshore structures. For heavy vertical loads or huge lateral loads, multiple piles in the form of pile groups are essential.

The design of laterally loaded piles involves consideration of the unusually large ratio of lateral to vertical loads in various structures like offshore structures, high-rise buildings, windmills, and transmission towers. Hence interaction between the structure and the foundation elements needs to be analyzed properly. Pile response to the lateral load is very much dependent on the surrounding soil. Pile response and soil reaction are both linked to the flexibility of pile and soil stiffness. Pile-soil interaction is a complex phenomenon. The same pile exhibiting flexible behavior in stiff soil may show rigid behavior in soft soil. The commonly used approaches for non-linear static analysis of laterally loaded piles are p-y analysis, elastic continuum approach, and finite element analysis. Nonlinear p-y analysis ignores the continuous nature of the soil and replaces it with discrete springs. The soil reaction at a point is simply linked with pile displacement at a given point. The elastic continuum approach assumes a pile as a thin strip embedded in idealized elastic media. Finite element analysis can model heterogeneous material properties and nonlinear behavior in a more rational manner.

Nowkandeh and Choobbasti[1] investigated the axial compressive behavior of helical piles in clay as well as in sand. The numerical models in ABAQUS software were validated and the effect of soil disturbance during the installation of helical piles was determined. The ultimate bearing capacity of the pile was determined and compared with theoretical results. It was observed that the theoretical method overpredicted the ultimate bearing capacity in medium and dense sand. The helical pile group with a square pattern was also analyzed and it was revealed that the shape of the block failure mechanism was different in clay and sand. A new theoretical method to calculate the ultimate bearing capacity of the helical pile group was suggested. Hassan et al.[2] studied the effect of the addition of polyethylene (PE) and polypropylene (PP) fibers on the geotechnical properties of soil. Four fiber contents (1%, 2%, 3%, and 4%) of the weight of the soil were used during the study. The lengths of the fibers were 1.0 cm and 2.0 cm. It was observed that the maximum dry density and optimum moisture content of soil decreased with the addition of fibers. There was a significant improvement in the unconfined compressive strength of soil by 76.4 % and 96.6 % for both lengths of PE fibers and 57.4% and 73 % for both lengths of PP fibers, respectively. In addition, 4 % fiber content was observed to be optimum in all cases during the California bearing ratio test. Ates Bayram and Sadoglu Erol[3] performed extensive numerical and experimental studies on pile groups to determine pile group efficiency. The tests were conducted in sand with different relative densities. The pile spacing and L/D ratio were also varied and their effect on pile group efficiency was investigated. The group efficiency of driven piles in cohesionless soil ranged from 1.31 to 1.66. A technique based on pile-pile interaction factors was proposed by Li and Deng[4] to estimate the settlement of the pile group in linear viscoelastic soil. The study was conducted on 2×2 and 3×3 pile groups. It was observed that the pile–pile-interaction factors increased with the increase of the pile-soil elastic modulus ratio and L/D ratio but decreased with the increase of the distance-to-diameter ratio. The predicted results deviated from field data by 14.9% and the correlativity coefficients R2 were greater than 0.9223. Khatti et al.[5] introduced an optimum performance soft computing model by comparing deep and hybrid learning models to predict pile group settlement. Sixteen performance databases were collected from the literature. Out of them, model MS23 was found to be best. Along with compression index, void ratio, and density, the problematic collinearity level significantly influenced the performance and accuracy of the deep learning model. Hamed et al.[6] studied the behavior of piles in response to axial compressive load. Numerical analysis was carried out in Plaxis 3D software and compared with experimental results. The parametric study revealed that the axial load-carrying capacity of a single pile increases with the increase in pile length and wall thickness. Dina et al.[7] established a correlation between the measured coefficient of variation of lateral subgrade reaction with depth (f) and both recommended values in codes and the elastic modulus of soil (E). Four full-scale pile load tests were constructed using FEM in different soil profile sites. E and f were found to be related logarithmically. Georgia Efthymiou and Christos Vrettos[8] reported a study on the response of pile group and piled raft foundations excited by a stationary or moving harmonic vertical point load acting on a soil surface. The soil was modeled as a linear elastic continuum with hysteretic damping. It was found that a stationary load located on a moving load path at the shortest distance from the pile group is a good approximation of a harmonic load traveling with a constant speed parallel to the pile group.

Ates Bayram and Sadoglu Erol[9] conducted experiments in sand to investigate the vertical stress increments below the piled raft foundation. The model composite piles made up of steel and concrete having diameters of 20 mm were used. The lengths of the piles were 200 mm and 300 mm. A Steel plate of size 160 x 160 mm in plan and 6 mm thick was used as a raft. The stresses at a distance of 2.5D, 5D, and 7D below the center of the piled raft foundation were measured. The experimental results were compared with numerical analyses in ABAQUS software. It was concluded that piles raft foundations transfer loads to the deep strata with the help of piles. The vertical stress increments were found to reduce downward from the pile tip. But they decreased with an increase in the relative density at the same loads. Similar experiments were conducted by Ates Bayram and Sadoglu Erol[10] on a single pile. In addition to vertical stress increments, the strain distribution along the depth was also investigated. Ates Bayram and Sadoglu Erol[11] investigated and compared the bearing capacity and settlement of only raft and piled raft foundations in loose sand. The tests were conducted on a model raft and a model piled raft. The results obtained can serve as a reference for the approximate estimation of bearing capacity and settlement of driven piles in sand. Ates Bayram and Sadoglu Erol[12] investigated experimentally, the influence of design parameters of piled raft foundations in sand like pile spacing, pile diameter, pile length, and relative density. It was revealed that with the increase in pile spacing, the bearing capacity of the piled raft foundation increased up to a certain value and then decreased. The optimum spacing of the piles was four times the diameter of the pile.

Using the p-y technique, Mukherjee and Dey[13] examined the response of a fixed-headed single pile subjected to lateral load in stratified soil consisting of alternate layers of clay and sand. Non-linear p-y curves using OASYS ALP v19.2 were elucidated. The study was conducted for piles of different diameters and lateral pile capacity moment and length of fixity were estimated. Yu et al.[14] evaluated and contrasted six current initial stiffness models from the standpoint of robust design. Several goals were taken into consideration, including robustness in design, economics, and safety. A simplified approach to design piles subjected to lateral load was proposed. Deb and Pal[15,16] presented a numerical study in ABAQUS 3D for three different pile group configurations in a square arrangement such as 3×3 piled raft, 4×4 piled raft, and 5×5 piled raft. The piles were embedded in cohesive soil underlain by sand. The effect of the thickness of the clay layer was investigated. The effect of pile positioning on pile response was also observed. Prediction models were developed. According to the parametric analysis, adding piles could regulate the differential and uniform settlement. Nazeran and Hosseinina[17] proposed a technique for laterally loaded pile groups in sandy soil that uses the idea of two-phase material to substitute a pile group with an equivalent single pile. Linear elastic behavior and the perfect bonding hypothesis were ascribed. The results showed good agreement with full-scale and centrifuge experimental results. Twenty-three experiments were carried out in sand on a pile group situated near a slope by Khati and Sawant[18]. The static lateral load was applied. The relative density of sand, the slope of the ground, and the distance of the pile group from the crest were changed during tests. In each test, the maximum bending moment and lateral displacement of the pile group were observed. As a basis of comparison, the response of the pile group in horizontal ground was also studied. It was discovered that for the pile group close to the slope, the maximum bending moment and lateral displacement significantly increased. The behavior became closer to that of the ground-level case as the pile group's distance from the slope rose. The p-y curves, p-multipliers, and reduction factors were also developed for the pile group near the slope. A 3D pile element model that can stimulate the behavior of piles under complicated loads in 3D space was created by Li et al.[19]. Since soil attributes were directly included in element formation, soils were not explicitly modeled. Pal D. et al.[20] assessed the p-y response of a laterally loaded single pile embedded in two-layered cohesionless substrata with the inclined interface. The tool of finite element method was used during the numerical analysis. Two cohesionless soil layers with an upper layer relatively weaker than the underlying stratum were considered and the inclination of the wedge was considered varying along the direction of the lateral load. It was observed that the interface inclination angle, the direction of the loading, and length to diameter ratio of the pile, significantly influenced the response of the laterally loaded pile. The effect of the strength and stiffness of multilayered strata on the response was also investigated. Bariker P. et al.[21] performed a series of small-scale model experiments for long piles with fins, embedded in c – φ soil. The outcomes were supported by numerical studies. Investigations were conducted on the impact of fin factors on the lateral resistance of finned piles, including fin orientation, length, width, position, eccentricity of load, and embedment in pile cap. The material cost-benefit study was also performed which clearly indicated that finned pile is a cost-effective alternative to large diameter regular piles. Babu S. Chawhan et al.[22] reported the results of experiments carried out on laterally loaded stainless steel piles and groups embedded in multilayered cohesionless soil. Piles with slenderness ratios 25, 30, and 38 were tested. The outcomes were validated with numerical models in Solid Works 2D software and found in good agreement. Riu He[23] proposed a novel semi-analytical model for laterally loaded piles. The input required is only two soil parameters, the shear modulus of soil and the reference shear strain at half the initial modulus. It was validated with nine existing studies. It requires less computational time, comparable with the p-y model, and has almost the same accuracy as the FEM model.

From the literature review, it can be concluded that though experimental, analytical, and numerical work is reported to find the response of laterally loaded pile and pile groups, the elastoplastic constitutive models are used to represent the behavior of soil in a few numerical studies. Also, the results obtained using different elastoplastic constitutive models like Von-Mises, Mohr-Coulomb, and both forms of Drucker-Prager models are rarely compared. Although nonlinear p-y analysis is a commonly used approach, finite element method (FEM) has been used for the analysis of laterally loaded piles in recent years. In this method, any element can be assigned with the property of any material. Complex boundary conditions or complicated soil layers can be handled. It can model the continuity of soil, nonlinearity of soil, and behavior at the pile-soil interface.

The laterally loaded pile behavior is affected by the non-linear behavior of soil. In the present study, a 3-D FEA program has been developed for the analysis of a pile group. The entire software program is prepared in FORTRAN 90. 3-Disoparametric continuum elements have been used to represent soil and pile media. The pile and pile cap have been modeled using twenty-node continuum elements having quadratic shape functions as they are suitable to model the medium with bending-dominated deformation. Eight node continuum elements having linear shape functions have been used to model the soil as they are suitable to model the medium with shear-dominated deformation. The pile is assumed to be linear elastic throughout the analysis. Soil is assumed to behave elasto plastically according to the different yield criteria. At the pile-soil interface, sixteen node interface elements have been employed to simulate the stress transfer. For these elements, the value of normal stiffness is assumed very high and the value of tangential stiffness is assumed very low. The interface element also helps in accounting for the pile-soil gap.

2 Material and Methodology

2.1 Constitutive Model

The materials used in the present study are reinforced concrete and soil. Piles are made of reinforced concrete and treated as linear elastic throughout the analysis. The soil is represented as elastoplastic material. The post-yielding behavior of soil is represented using the theory of plasticity. According to this theory, material behavior is stress path dependent. Hence the constitutive relationships are incremental in nature. Nonlinear constitutive soil behavior can be represented by considering the following essential features:

1. Yield function that distinguishes between an elastoplastic and pure elastic condition
2. A plastic potential function that, using a flow rule, indicates the direction of plastic strains at each stress state following yielding.
3. A rule of hardening/softening that specifies how the yield function changes when the plastic stresses change

In the present study, Von-Mises, Mohr-Coulomb, and Drucker-Prager models are being considered to represent nonlinear soil behavior. These models are modified in suitable form by Nayak and Zienkiwicz[24] and Viladkar et al.[25]. It gives a generalized approach to use them in FEA and also simplifies the computations. The yield function and plastic potential function are stated by the same function (associative flow rule). It yields a symmetric stiffness matrix. This enables a reduction in storage space and time for computation. Different yield criteria used in the analysis are discussed in subsequent paragraphs. They are expressed as a function of stress invariants. The stress invariants are expressed in terms of stress components as,

$$J_1 = \sigma_x + \sigma_y + \sigma_z$$

$$J_2 = \sigma_x\sigma_y + \sigma_y\sigma_z + \sigma_z\sigma_x + \tau_{xy}^2 + \tau_{yz}^2 + \tau_{xz}^2$$

$$J_3 = \sigma_x\sigma_y\sigma_z + 2\tau_{xy}\tau_{yz}\tau_{xz} - \sigma_x\tau_{yz}^2 - \sigma_y\tau_{xz}^2 - \sigma_z\tau_{xy}^2 \tag{1}$$

In addition, the second deviatoric stress invariant is given by,

$$J_2^{'} = \frac{1}{6}\left(\sigma_x - \sigma_y\right)^2 + \frac{1}{6}\left(\sigma_y - \sigma_z\right)^2 + \frac{1}{6}\left(\sigma_z - \sigma_x\right)^2 + \tau_{xy}^2 + \tau_{yz}^2 + \tau_{xz}^2 \tag{2}$$

In an elasto-plastic state, the relation between incremental strains {De} and incremental stresses, {Dσ} is given below.

$$\{\Delta\sigma\} = [D]_{ep}\{\Delta\varepsilon\} \tag{3}$$

where, [D$_{ep}$] is an elasto-plastic constitutive matrix.

$$[D]_{ep} = [D] - \frac{[D]\left\{\frac{\partial P}{\partial \sigma}\right\}\left\{\frac{\partial F}{\partial \sigma}\right\}^T [D]}{A + \left\{\frac{\partial F}{\partial \sigma}\right\}^T [D]\left\{\frac{\partial P}{\partial \sigma}\right\}} \tag{4}$$

Where, [D] = elastic constitutive matrix, P and F are plastic potential function and yield function respectively. For perfectly plastic material, A = 0[26].

Using chain rule, the flow vector, $a = \{\vartheta F/\vartheta\sigma\}$, can be written as:

$$a = \frac{\partial F}{\partial p'}\frac{\partial p'}{\partial \sigma} + \frac{\partial F}{\partial J}\frac{\partial J}{\partial \sigma} + \frac{\partial F}{\partial \theta}\frac{\partial \theta}{\partial \sigma} \tag{5}$$

It can also be expressed as explained by Nayak and Zienkiwicz[24]:

$$a = C_1 a_1 + C_2 a_2 + C_3 a_3 \tag{6}$$

$$where,\ C_1 = \frac{\partial F}{\partial p'}; C_2 = \frac{\partial F}{\partial J}; C_3 = \frac{\partial F}{\partial \theta}\ and\ a_1 = \frac{\partial p'}{\partial \sigma}; a_2 = \frac{\partial J}{\partial \sigma}; a_3 = \frac{\partial \theta}{\partial \sigma}$$

$$\begin{aligned} a_1 &= \tfrac{\partial p'}{\partial \sigma} = \tfrac{1}{3}\begin{bmatrix}1 & 1 & 1 & 0 & 0 & 0\end{bmatrix}^T \\ a_2 &= \tfrac{\partial J}{\partial \sigma} = \tfrac{1}{2J}\begin{bmatrix}\sigma_x - p' & \sigma_y - p' & \sigma_z - p' & 2\tau_{xy} & 2\tau_{yz} & 2\tau_{zx}\end{bmatrix}^T \\ a_3 &= \tfrac{\partial \theta}{\partial \sigma} = \tfrac{\sqrt{3}}{2J^3 cos3\theta}\left(3\tfrac{J_3}{J}\tfrac{\partial J}{\partial \sigma} - \tfrac{\partial J_3}{\partial \sigma}\right) \end{aligned}$$

$$where,\ J_3 = \begin{vmatrix} \sigma_x - p' & \tau_{xy} & \tau_{zx} \\ \tau_{xy} & \sigma_y - p' & \tau_{yz} \\ \tau_{zx} & \tau_{yz} & \sigma_z - p' \end{vmatrix} \tag{7}$$

2.1.1 Von-Mises Yield Criterion

In 3-D principal stress space, Tresca yield function plots a regular hexagon with corners in deviatoric plane[26]. This leads to singularities and causes numerical ill conditioning in three dimensional analyses. In finite element computations additional efforts are required to deal with them. Von Mises yield criteria plots a circular cylinder with central axis coinciding with space diagonal when represented in principal stress space. Von Mises yield function is expressed in terms of J'_2 and material constant K as,

$$\sqrt{3J_2^{'}} = K \tag{8}$$

2.1.2 Mohr-Coulomb Yield Criterion

The governing expression for Mohr-Coulomb criterion is,

$$\frac{1}{3}J_1 sin\left(\varphi\right) + J_2^{'\frac{1}{2}}\left(\frac{cos\left(\theta\right) - sin\left(\theta\right)sin\left(\varphi\right)}{\sqrt{3}}\right) - c.cos\left(\varphi\right) = 0 \tag{9}$$

In which, $\theta = \frac{1}{3}sin^{-1}\left(\frac{-3\sqrt{3}J_3}{2\left(J_2^{'}\right)^{\frac{3}{2}}}\right)$ ($-30^{\circ} \leq \theta \leq 30^{\circ}$)

It also possesses angular vertices due to which the partial derivatives of yield and plastic potential functions which are required to define elastoplastic constitutive matrix [D_{ep}], are not uniquely defined at corners[26].

2.1.3 Drucker-Prager Yield Criterion

Drucker and Prager modified the Von-Mises yield criteria and proposed an approximation to the Mohr-Coulomb law. By adding a new term to the von Mises formula, the impact of the hydrostatic stress component on yielding was added. Its expression is as follows:

$$\alpha J_1 + \sqrt{J_2^{'}} = K \tag{10}$$

where, a and K are material constants, which may be related to Coulomb's material constants c and j[27].

In order to make the Drucker-Prager circle coincide with the inner (Equation (11a)) and outer (Equation (11b)) apices of the Mohr-Coulomb hexagon at any section, it can be shown that[26]:

$$\alpha = \frac{2sin\varphi}{\sqrt{3}\left(3 + sin\varphi\right)} \;\&\; K = \frac{6ccos\varphi}{\sqrt{3}\left(3 + sin\varphi\right)} \tag{11a}$$

$$\alpha = \frac{2sin\varphi}{\sqrt{3}\left(3 - sin\varphi\right)} \;\&\; K = \frac{6ccos\varphi}{\sqrt{3}\left(3 - sin\varphi\right)} \tag{11b}$$

2.2 Nonlinear Algorithm to Calculate Displacement Due to Static Load

The static load is divided into ten equal parts and each part is applied separately and steps given below are followed for each part. The stiffness matrix, [K] is maintained constant throughout the process. The following procedure is to be applied for nonlinear analysis once each tenth of a load is applied.

1. For the first cycle of each equal part, apply one-tenth value of the total load as incremental load {DF}. For the next cycles, apply {DF} obtained in step (6) as incremental load. The following equations solved to obtain incremental displacement, $\{\Delta u\} = [K]^{-1}\{\Delta F\}$.

2. Incremental displacement, Δu, is to be added to displacement obtained in the previous increment u_{i-1}, and displacement for an i^{th} increment is obtained as
$\{u\}_i = \{u\}_{i-1} + \{\Delta u\}$'.

3. The value of a number of yielded elements, y_e, is set to be equal to zero.

4. The value of a number of yielded points, y_p, is set to be equal to zero for each element.

5. From global incremental displacement vector Δu, elemental incremental displacement vector, $\{\Delta\delta\}$ is to be selected.

6. The incremental stress, {$\Delta\sigma$} and total stress for ith increment, {σi}, for all 27 gauss points is obtained using relations given below:

{$\Delta\sigma$} = [D] [B] {$\Delta\delta$} and {σi} = {σi-1} + {$\Delta\sigma$}

where, {σi-1} is the total stress at i-1th iteration. {σi} is checked with yield stress. If the Gauss point under consideration is not yielded, the next Gauss point is considered. Otherwise, y$_p$ is set equal to y$_{p+1}$ and extra stress than the yield stress. {$\Delta\sigma$}extra is calculated using the following relation:

{$\Delta\sigma$}extra = [D – Dep] {$\Delta\varepsilon$}

The total stress is kept at the yield level by following the equation,

{σi} = {σi} - {$\Delta\sigma$}extra

The additional load vector {ΔF} is obtained as below and is applied in the next iteration.

$$\{\Delta F\}^e = \iiint_V [B]^T \cdot \{\Delta\sigma\}_{ext} dV$$

This procedure is repeated for all Gauss points of the element.

If y$_p$> 0, ye is set equal to y$_{e\,+\,1}$.

Step (4) to (6) is repeated for all the elements.

7. If y$_e$ = 0, it means that no element is yielded and the next one-tenth part of the load is applied.

8. If ye > 0, then convergence is checked using the following criteria:

$$e_d = \frac{\left(\sqrt{\sum(q_i)^2} - \sqrt{\sum(q_{i-1})^2}\right)}{\sqrt{\sum(q_i)^2}}$$

Where, e$_d$ = displacement norm, q$_i$ and q$_{i-1}$ are total displacement at the ith and i-1th iteration.

9. If the convergence criterion is observed, then the next one-tenth of the load is applied. Else procedure from step (1) to step (9), is repeated till the convergence of the displacements.

2.3 Validation

The results obtained in the present analysis using the Von Mises yield criterion have been validated with experimental works reported in the literature. Ismael and Klym[27] reported the pile load test data for the soil in Ontario. The test was conducted on a concrete pile of 60 in (1.52m) and 39 ft (12.0 m) length. One foot (0.30 m) length of the pile was above ground-line. The flexural rigidity, EI, of the pile, was 93´1010 lb-in2(2.675×106 kN.m2). The over-consolidated clay having cohesion of 2000 lb/ft2 (96.0 kPa) was present. Lateral deflections of the pile reported by Ismael and Klym[28] and obtained by the present analysis are presented in Figure 1 At higher load levels, a reasonably good agreement is observed.

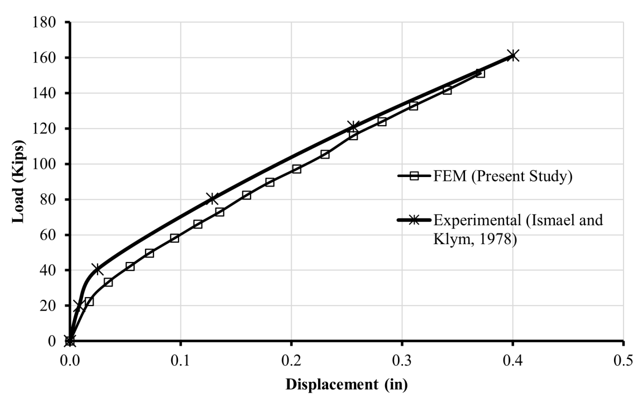

Fig 1. Validation of finite element analysis results with experimental work

3 Results and Discussion

Initially, a convergence study was carried out to fix the appropriate boundary distance. A typical mesh convergence study has been carried out on 3×3 pile group configuration (diameter, D=1.0 m, elasticity modulus of soil, Es= 20000 kPa, length to diameter ratio, L/D=20, spacing to diameter ratio, s/D=3) to decide the size of the mesh for finite element analysis. It has been observed that beyond 14D, there is no change in the predicted displacement for a given case, therefore for all the analyses the mesh is extended by 14 times the diameter of the pile (14D) on all the sides of the pile group from the outer edge of exterior pile in the group. A convergence study revealed a boundary distance of 14D from the edge of the pile cap is sufficient to avoid boundary effect. Total Lateral deflection at the center of the pile cap of the 3×3 pile group for each increment has been studied using different yield criteria and influencing parameters. Different yield criteria such as Von Mises, Mohr-Coulomb, and Drucker-Prager have been employed. The effect of two Drucker-Prager yield criteria (yield surface inscribing and circumscribing Mohr-Coulomb yield surface) are being investigated.

It is assumed that the pile remains elastic throughout the analysis. The soil is behaving elasto-plastically according to selected yield criteria. The lateral load has been applied in 10 equal parts. In each increment of load, initial stresses in the soil elements have been calculated using elastic constitutive relations. They are compared with the yield stress of chosen yield criteria. The extra stress, if any, is converted into force and applied again. This iterative procedure is carried out until a satisfactory convergence is achieved. Undrained analysis is carried out for square 3×3 bored pile group embedded in homogeneous clay under the action of 4000kN horizontal load for parameters defined in Table 1. The ground water table is assumed very deep.

Table 1. Properties of pile and soil for parametric study

Soil properties	
Elasticity Modulus, E_s	10000 kPa to 40000 kPa
Unit Weight, γ_s	18 kN/m^3
Poisson's ratio, μ_s	0.4
Cohesion, c	100 kPa
Angle of internal friction, ϕ	0
Pile properties	
Elasticity Modulus, E_p	25 GPa
Pile diameter, D	0.6 m, 0.7 m, 0.8 m, 0.9 m and 1.0 m
Poisson's ratio, m_p	0.3
length to diameter (L/D) ratio	10, 15, 20 and 25
Unit Weight, γ_p	25 kN/m^3
spacing to diameter (s/D) ratio	2, 3, 4, 5 and 6
Thickness of Pile cap, t_p	0.5 m
Interface element	
Normal stiffness, K_n	1.0×10^6kN/m^3
Tangential stiffness, K_s	1000 kN/m^3

3.1 Effect of Yield Criteria

Figure 2 **a** shows the variation of displacement with load using different yield criteria for L/D = 20, s/D = 3, Es = 20000 kPa, and D = 1 m. It is observed that the difference between the displacements is small at lower load but it increases with an increase in load. At maximum load, the Drucker-Prager inner yield criterion predicts the highest displacement and the Mohr-Coulomb criterion predicts the lowest displacement. The pile top displacements for maximum load using all yield criteria are summarized in Table 2 for comparison. Figure 2 **b** depicts the variation in maximum bending moment with load using different yield criteria. Values of the maximum bending moment are lowest for Mohr-Coulomb criteria and highest for Von Mises yield criteria. As compared to linear response, the increase in the maximum bending moment is only 14.8% for Mohr-Coulomb criteria followed by 71.8% for Drucker-Prager outer, 104.8% Drucker-Prager inner, and 109% for Von Mises yield criteria. The effect of all-around stress is clearly noticeable. Von Mises yield criteria being independent of the first stress invariant exhibits lower yield strength. For different yield criteria (Von Misses, Drucker-Prager outer, Drucker-Prager inner, and Mohr-Coulomb), the difference between the displacements of the pile is small at lower loads but it increases with an increase in load. At the maximum load, out of two Drucker-Prager models, the Drucker-Prager inner yield criterion yields 24% more displacement than the Drucker-Prager outer yield criterion. This is due to the larger size Drucker-Prager outer yield criterion which allows less yielding of soil at given loads.

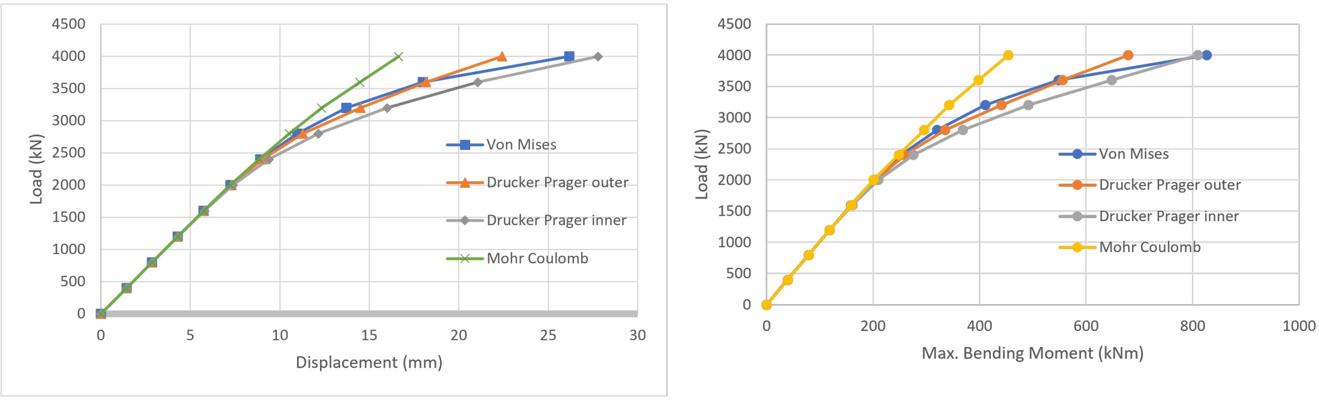

Fig 2. (a) Load-displacement comparison for different yield criteria (b) Load-maximum moment comparison for different yield criteria

Table 2. Comparison of displacement for different yield criteria

Yield Criteria	Displacement (mm)
Von Misses	26.17
Drucker-Prager outer	22.41
Drucker-Prager inner	27.79
Mohr-Coulomb	16.63

3.2 Effect of Pile Spacing

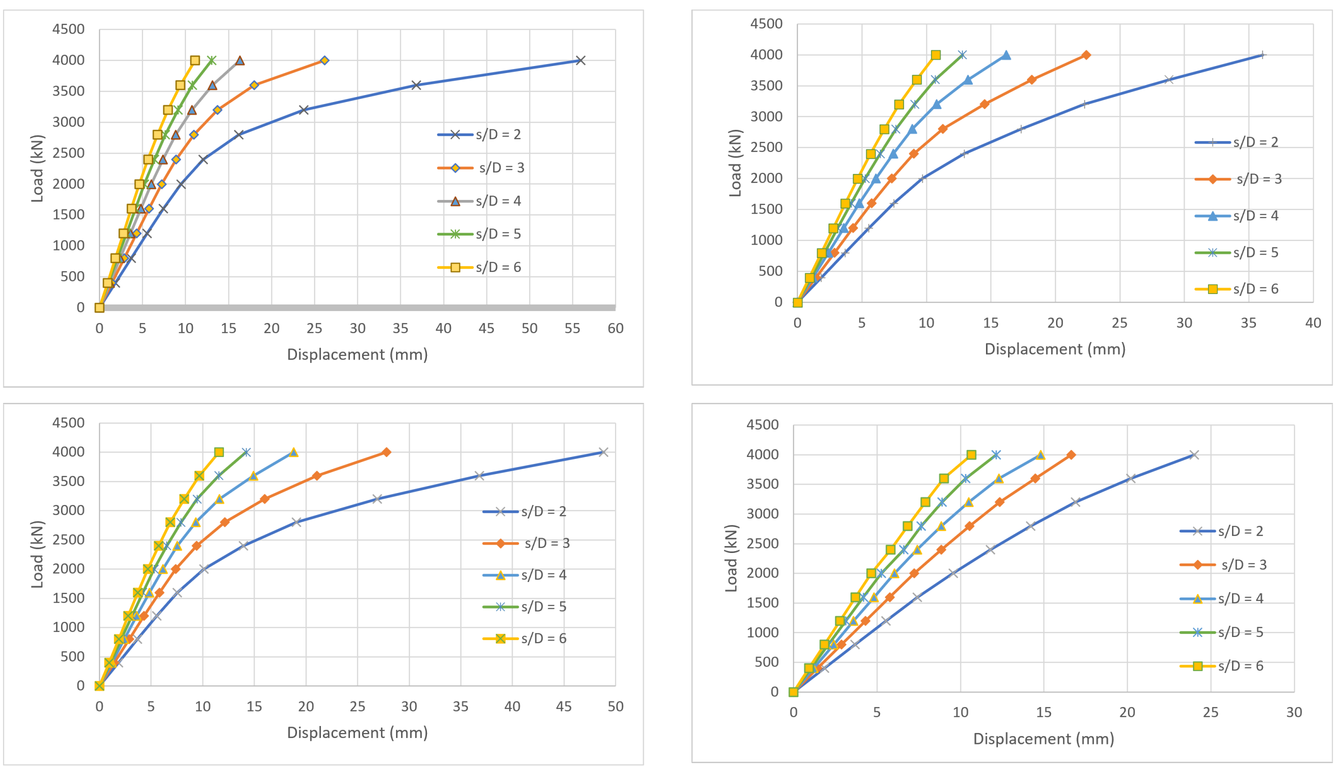

Fig 3. (a) Load-displacement comparison for different s/D ratio using Von Mises yield criteria (b) Load-displacement comparison for different s/D ratio using Drucker-Prager outer yield criteria (c) Load-displacement comparison for different s/D ratio using Drucker-Prager inner yield criteria (d)Load-displacement comparison for different s/D ratio using Mohr-Coulomb yield criteria

Table 3. Comparison of displacement for different pile spacing and yield criteria

Yield Criteria	s/D =2	s/D =3	s/D =4	s/D =5	s/D =6
Von Misses	55.92	26.17	16.31	13.03	11.11
Drucker-Prager outer	36.08	22.41	16.20	12.80	10.70
Drucker-Prager inner	48.84	27.79	18.79	14.22	11.58
Mohr-Coulomb	24.01	16.63	14.80	12.15	10.65

Figure 3**(a)**-**(c)** shows the variation of displacement with load for different yield criteria using different s/D ratios for L/D = 20, Es = 20000 kPa, and D = 1 m. It is observed that in all yield criteria, the pile displacement reduces with an increase in pile spacing. This is because the overlapping zone reduces with an increase in spacing. Also, more soil is available for passive resistance. The pile top displacements for maximum load using all yield criteria are summarized in Table 3 for comparison. As the s/D ratio increases from 2 to 6, the pile displacement reduces by 80.13% in Von Misses, 70.3% in Drucker-Prager outer, 76.68% in Drucker-Prager inner and 55.64% in Mohr-Coulomb yield criteria. This is due to the lesser overlapping of pressure zones and higher availability of passive resistance of soil at higher pile spacing.

3.3 Effect of Soil Modulus, Diameter, and L/D Ratio

Effects of soil modulus, diameter, and L/D ratio have been investigated by incorporating the Von Mises yield criterion. Default parameters are Es = 20000 kPa, L/D= 20, s/D = 3 and D = 1m. To examine the effect of one particular parameter, only that parameter has been varied and others have been assigned to default values. Pile top displacements y_{top} can be expressed in non-dimensional form as deflection influence factors $I_{\rho H}$ as defined by Poulos and Davis as

$$I_{\rho H} = \frac{y_{top} E_S T}{H} \; where \; T = \sqrt[4]{\frac{EI}{E_S}}$$

The pile top displacements y_{top} and I_{rH} for maximum load using Von Mises yield criteria have been summarized in Table 4 for comparison for different variations (E_s, D, and L/D).

Table 4. Comparison of displacement for different variations using Von Mises yield criterion (s/D =3)

Other Parameters	Variable	1	2	3	4	5
(D =1 m and L/D= 20)	E_s (MPa)	20	30	40	50	60
Top Horizontal Displacement (mm)		26.16	21.11	18.14	16.23	14.88
I_{rH}		0.3661	0.4004	0.4269	0.4516	0.3661
(E_s= 20 MPa and L/D= 20)	D (m)	0.6	0.7	0.8	0.9	1.0
Top Horizontal Displacement (mm)		242.6	124.25	66.79	39.47	26.17
I_{rH}		2.0370	1.2171	0.7477	0.4971	0.3662
(E_s= 20 MPa and D=1.0 m)	L/D	10	15	20	25	
Top Horizontal Displacement (mm)		33.62	27.37	26.17	25.58	
I_{rH}		0.4705	0.3830	0.3662	0.3580	

Figure 4 depicts the variation of displacement with load using the Von Mises yield criterion for different soil modulus for L/D = 20, s/D = 3, and D = 1m. It has been observed that the pile displacement reduces with an increase in soil modulus. As the elastic modulus of soil increases from 20000 kPa to 60000 kPa, the pile displacement decreases by 43.12% in Von Mises yield criteria. This is because of an increase in the stiffness of soil. Also, higher elastic modulus will result in lesser strains and yielding of soil.

Figure 5 shows the variation of displacement with load for different pile diameters for L/D= 20, s/D = 3 and Es = 20000 kPa. It has been noticed that the pile displacement reduces with an increase in pile diameter. This is because a pile with a higher diameter mobilizes more soil and hence achieves higher lateral resistance. Also, the moment of inertia and rigidity of the pile increases. The pile top displacements for maximum load using the Von Mises yield criterion are summarized in Table 4 for comparison. As the pile diameter increases from 0.6 m to 1.0 m, the pile displacement reduces by 82.73% in the Von Mises yield criterion.

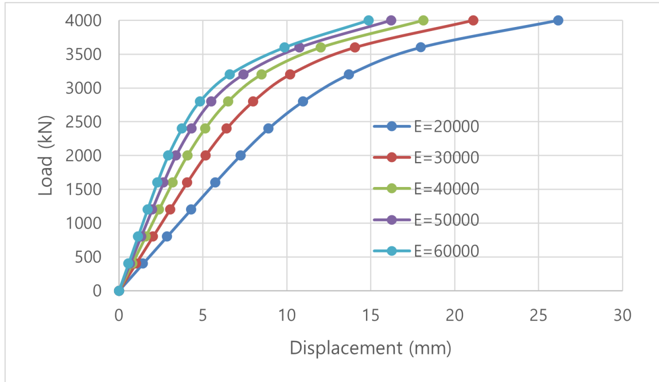

Fig 4. Load-displacement comparison for different soil modulus using Von Mises yield criteria

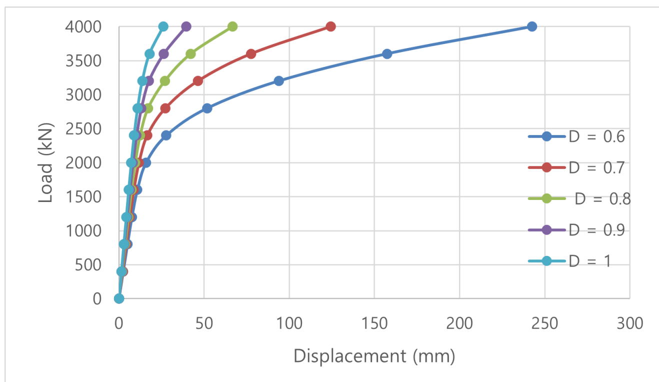

Fig 5. Load-displacement comparison for different diameter using Von Misesyield criteria

Figure 6 compares the variation of displacement with load using the Von Mises yield criterion for different L/D ratios, for, s/D = 3 and Es = 20000 kPa and D = 1 m. It has been noticed that the pile displacement reduces marginally with an increase in the L/D ratio. Though the pile tends to be flexible with an increase in length, the fact that it mobilizes more soil is found governing. The pile top displacements for maximum load using Von Mises yield criteria have been summarized in Table 4 for comparison. As the L/D ratio increments from 10 to 25, the reduction in pile displacement is 23.91% in Von Mises yield criteria. This may also be attributed to greater mobilization of passive resistance of soil by greater length. However, this difference is found marginal at the L/D ratio of more than 15.

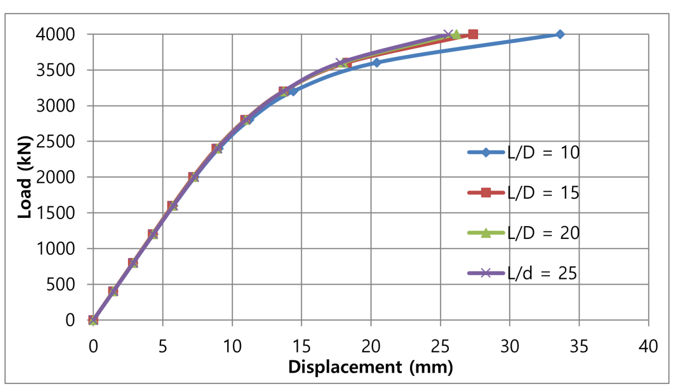

Fig 6. Load-displacement comparison for different L/D ratio using Von Misesyield criteria

4 Conclusions

An attempt has been made to analyze the response of a 3 x 3 pile group subjected to a lateral load of 4000 kN using 3D finite element analysis. The in-house software in FORTRAN 90 is developed. The response is found in terms of lateral displacement and maximum bending moment developed. The pile is assumed to be linearly elastic throughout the analysis. The different elastoplastic models like Von – Mises, Mohr - coulomb, Drucker–Prager (outer), and Drucker–Prager (inner) are used to model soil behavior which is rare. The response obtained by these models is compared. The parametric study emphasizing the influence of geometrical and material parameters is also carried out. The conducted study's conclusions are as follows:

- For different yield criteria, the difference between the displacements of the pile group is small at lower loads but it increases with an increase in load. At the maximum load, out of two Drucker-Prager models, the Drucker-Prager inner yield criterion predicts 24% more displacement than the Drucker-Prager outer yield criterion. Among the Von – Mises, Mohr-Coulomb, Drucker–Prager (outer), and Drucker–Prager (inner) criteria, the Mohr-Coulomb criterion predicts the lowest displacement. The study envisaged a clear effect of all-around stress-dependent yield criterion on lateral response.
- As the s/D ratio increases from 2 to 6, the decrease in pile displacement reduces by 80.13% in Von Misses, 70.3% in Drucker-Prager outer, 76.68% in Drucker-Prager inner, and 56.62% in Mohr-Coulomb yield criteria. This is because there is more passive resistance available with greater pile separation and fewer pressure zone overlaps. With the increase in the placing, the plastic zone between two piles minimizes due to lesser overlapping of stresses. This in turn reduces the effect of yield criteria.
- As the elastic modulus of soil increases from 20000 kPa to 60000 kPa, the pile displacement decreases by 43.12% in the Von Mises yield criterion. This may be attributed to higher soil stiffness causing lesser strains and yielding of soil due to increased stiffness of soil.
- Because of the increased mobilization of soil's passive resistance with a bigger pile diameter, the Von Mises yield criteria show that the pile displacement decreases by 82.73% as the pile diameter grows from 0.6 m to 1.0 m.
- As the L/D ratio increments from 10 to 25, the reduction in pile displacement is 23.91% in Von Mises yield criteria. However, this difference is found marginal at the L/D ratio of more than 15. Below the location of the maximum bending moment, the effect of the top lateral load is minimal.

References

1) Nowkandeh MJ, Choobbasti AJ. Numerical study of single helical piles and helical pile groups under compressive loading in cohesive and cohesionless soils. *Bulletin of Engineering Geology and the Environment*. 2021;80(5):4001–4023. Available from: https://dx.doi.org/10.1007/s10064-021-02158-w.
2) Hassan HJA, Rasul J, Samin M. Effects of Plastic Waste Materials on Geotechnical Properties of Clayey Soil. *Transportation infrastructure Geotechnology*. 2021;8(3):390–413. Available from: https://doi.org/10.1007/s40515-020-00145-4.
3) Ateş B, Şadoğlu E. Experimental Investigation for Group Efficiency of Driven Piles Embedded in Cohesionless Soil. *KSCE Journal of Civil Engineering*. 2023;27:5123–5134. Available from: https://doi.org/10.1007/s12205-023-1580-0.
4) Li L, Deng Y. Analysis of Settlement of Group Pile Foundation in Linear Viscoelastic Soil. *Advances in Civil Engineering*. 2023;3207304:1–12. Available from: https://doi.org/10.1155/2023/3207304.
5) Khatti J, Samadi H, Grover KS. Estimation of Settlement of Pile Group in Clay Using Soft Computing Techniques. *Geotechnical and Geological Engineering*. 2024;42:1729–1760. Available from: https://doi.org/10.1007/s10706-023-02643-x.
6) Hamed M, Emirler B, Canakci H, Yildiz A. 3D Numerical Modeling of a Single Pipe Pile Under Axial Compression Embedded in Organic Soil. *Geotechnical and Geological Engineering*. 2020;38:4423–4434. Available from: https://doi:10.1007/s10706-020-01299-1.
7) Dina MO, Ahmed ME, Hisham AM. Evaluating the Lateral Subgrade Reaction of Soil using Horizontal Pile Load Test Results. *Ain Shams Engineering Journal*. 2022;13(5):1–15. Available from: https://doi.org/10.1016/j.asej.2022.101734.
8) Georgia E, V C. Kinematic response of pile groups and piled rafts to a distant stationary or moving harmonic load via the FEM. . *Soil Dynamics and Earthquake Engineering*. 2024;176:108264–108264. Available from: https://doi.org/10.1016/j.soildyn.2023.108264.
9) Ateş B, Şadoğlu E. Experimental and Numerical Investigation for Vertical Stress Increments of Model Piled Raft Foundation in Sandy Soil. *Iranian Journal of Science and Technology*. 2022;46:309–326. Available from: https://doi.org/10.1007/s40996-021-00618-7.
10) Ates B, Şadoğlu E. Experimental and Numerical Investigation of Single Pile Subjected to Vertical Load in Sand. In: Proceedings of 3rd International Conference on Advanced Engineering Technologies. 2021. Available from: https://doi.org/10.1007/s40996-021-00618-7.
11) Ateş B, Şadoğlu E. Experimental Investigation of Pile Addition and Length on Bearing Capacity and Settlement of Rafts on Loose Sandy Soil. *Afyon Kocatepe University Journal of Science and Engineering*. 2021;21(2):399–407. Available from: https://doi.org/10.35414/akufemubid.863095.
12) Ateş B, Şadoğlu E. Experimental Investigation of Optimum Piles Spacing for Piled Raft Foundation in Sandy Soils. *Technical Journal*. 2021;32(1):10477–10494. Available from: https://doi.org/10.18400/tekderg.644885.
13) Mukherjee S, Dey A. Analysis of laterally loaded fixed headed single pile in multilayered soil using p-y approach. *Geotechnical Applications*. 2019;p. 41–50. Available from: https://doi.org/10.18400/tekderg.644885.
14) Yu Y, Shen M, Juang CH. Assessing initial stiffness models for laterally loaded piles in undrained clay: Robust design perspective. *Journal of Geotechnical and Geoenvironmental Engineering, ASCE*. 2019;(10):145–145. Available from: https://doi.org/10.1061/(asce)gt.1943-5606.0002074.
15) Deb P, Pal SK. Numerical analysis of piled raft foundation under combined vertical and lateral loading. *Ocean Engineering* . 2019;190. Available from: https://doi.org/10.1016/j.oceaneng2019.106431.

16) Deb P, Pal SK. Structural and geotechnical aspects of piled raft foundation through numerical analysis. . *Marine Georesources and Geotechnology*. 2021. Available from: https://doi.org/10.1080/1064119X.2021.1943083.
17) Nazeran N, Hosseinina ES. Two-phase approach for the analysis of laterally loaded pile groups in sandy soil. *International Journal of Geomechanics*. 2020;20(10). Available from: https://doi.org/10.1061/(ASCE)GM.1943-5622.0001821.
18) Khati B, Sawant V. Experimental Study of Laterally Loaded Pile Group in Square Arrangement near Sloping Ground. *International Journal of Geomechanics*. 2021;21(2):4020257–4020257. Available from: https://doi.org/10.1061/(ASCE)GM.1943-5622.0001911.
19) Li XY, Wan JH, Zhao HP, Liu SW. Three-dimensional analysis of nonlinear pile - soil interaction responses using 3 D pile element model. *International Journal of Geomechanics, ASCE*. 2021;21(8). Available from: https://doi.org/10.1061/(ASCE)GM.1943-5622.0002076.
20) Pal D, Dey A, Dasgupta K. Assessment of p-y response of a laterally loaded single pile embedded in two-layered cohesionless substrata with inclined interface. *International Journal of Geotechnical Engineering*. 2023;p. 1–13. Available from: https://doi.org/10.1080/19386362.2023.2297497.
21) Bariker P, Kolathayar S, Chandrasekaran SS. Lateral resistance of finned piles in c - φ soils : experimental investigations and numerical studies. *Indian Geotechnical Journal*. 2023;53(5):957–947. Available from: https://doi.org/10.1007/s40098-023-00748-x.
22) Babu S, Chawhan G, Vijapur, Girish KH, Patil S, Desai S, et al. Lateral load capacity of model piles on cohesionless soil at 3D pile spacing. *Journal of Basic Science and Engineering*. 2024;21(1):210–244. Available from: https://yjgkx.org/article/view/24.
23) He R. A novel semi-analytical model for laterally loaded pile. *Ocean Engineering*. 2024;306:1–17. Available from: https://doi.org/10.1016/j.oceaneng.2024.118084.
24) Nayak GC, Zienkiwicz OC. Convenient forms of stress invariants for plasticity. *Journal of the Structural Division ASCE*. 1972;98(4):949–954. Available from: https://doi.org/10.1016/j.oceaneng.2024.118084.
25) Viladkar MN, Noorzaei J, Godbole PN. Convenient Forms of Yield Criteria in Elasto Plastic Analysis of Geological Materials. *Computers & Structures*. 1995;54(2):327–364. Available from: https://doi.org/10.1016/0045-7949(94)E0199-C.
26) Potts DM, Zdravkovic L. Finite Element Analysis in Geotechnical Engineering. London, UK. Thomas Telford. 1999. Available from: https://wp.kntu.ac.ir/fz_kalantary/Source/.
27) Drucker DC, Prager W. Soil mechanics and plastic analysis on limit design. *Journal of Applied Mathematics*. 1952;10(2):157–165. Available from: https://doi.org/10.1090/QAM/48291.
28) Ismael NF, Klym TW. Behavior of rigid piers in layered cohesive soils. *Journal of Geotechnical and Geoenvironmental Engineering, ASCE*. 1978;106. Available from: https://doi.org/10.1061/AJGEB6.0000678.